PHYSICAL REVIEW B **85**, 054403 (2012)

Entanglement spectra of coupled $S = \frac{1}{2}$ spin chains in a ladder geometry

Andreas M. Läuchli[1,2,*] and John Schliemann[3,†]
[1]*Institut für Theoretische Physik, Universität Innsbruck, A-6020 Innsbruck, Austria*
[2]*Max-Planck-Institut für Physik komplexer Systeme, Nöthnitzer Strasse 38, D-01187 Dresden, Germany*
[3]*Institute for Theoretical Physics, University of Regensburg, D-93040 Regensburg, Germany*
(Received 28 June 2011; revised manuscript received 14 January 2012; published 1 February 2012)

We study the entanglement spectrum of spin-1/2 XXZ ladders both analytically and numerically. Our analytical approach is based on perturbation theory starting either from the limit of strong rung coupling, or from the opposite case of dominant coupling along the legs. In the former case we find to leading order that the entanglement Hamiltonian is also of nearest-neighbor XXZ form although with an, in general, renormalized anisotropy. For the cases of XX and isotropic Heisenberg ladders no such renormalization takes place. In the Heisenberg case the second-order correction to the entanglement Hamiltonian consists of a renormalization of the nearest-neighbor coupling plus an unfrustrated next-nearest-neighbor coupling. In the opposite regime of strong coupling along the legs, we point out an interesting connection of the entanglement spectrum to the Lehmann representation of single-chain spectral functions of operators appearing in the physical Hamiltonian coupling the two chains.

DOI: 10.1103/PhysRevB.85.054403 PACS number(s): 75.10.Jm, 03.67.−a

I. INTRODUCTION

In the past decade many-body physics has been substantially enriched by the concept of entanglement, whose extensive and systematic study originated in the field of quantum information theory.[1] In particular, the notion of the *entanglement spectrum*[2] has led to novel insights in the physics of various many-body systems. These include quantum Hall monolayers at fractional filling,[2–11] quantum Hall bilayers at filling factor $\nu = 1$,[12] spin systems of one[13–18] and two[19–21] spatial dimensions, and topological insulators.[22,23] Other topics recently covered encompass rotating Bose-Einstein condensates,[24] coupled Tomonaga-Luttinger liquids,[25] and systems of Bose-Hubbard[26] and complex paired superfluids.[27]

In Ref. 17 Poilblanc observed that chain-chain entanglement spectra in two-leg spin ladders are remarkably similar to the *energy* spectrum of a single Heisenberg chain. Furthermore he found that the fitted effective inverse temperature depends on the ratio of the leg to the rung couplings and vanishes in the limit of strong rung coupling. In a parallel study of entanglement spectra of quantum Hall bilayers at $\nu = 1$ one of the present authors observed a similarly striking analogy between the entanglement spectrum of a single layer and the energy spectrum of a single physical layer at $\nu = 1/2$.[12]

In this paper we study the entanglement spectrum of two coupled XXZ chains analytically in two limiting cases: (a) the case of strong rung coupling and (b) the case of weak rung coupling. In case (a) we find that the entanglement spectrum is described to leading order by an entanglement Hamiltonian of the XXZ form, albeit with an, in general, renormalized effective anisotropy (and thus independently reproducing the recently posted result of Ref. 18). For the particular cases of XX and Heisenberg ladders the anisotropy is unaltered, and we arrive at the conclusion that in these cases the entanglement Hamiltonian is indeed the physical Hamiltonian restricted to a single chain. Moreover, we derive explicit results for the next-to-leading order exhibiting deviations of the entanglement Hamiltonian from nearest-neighbor XXZ coupling. In case (b) we point out an interesting connection between the entanglement spectrum and the Lehmann representation of single-chain spectral functions of the operators contained in the physical Hamiltonian coupling the two chains.

We consider an XXZ spin-ladder Hamiltonian $\mathcal{H} = \mathcal{H}_0 + \mathcal{H}_1$ with

$$\mathcal{H}_0 = J_{\text{rung}} \sum_m \left[\frac{1}{2}(S^+_{m,1} S^-_{m,2} + \text{H.c.}) + \Delta S^z_{m,1} S^z_{m,2} \right],$$
$$\mathcal{H}_1 = J_{\text{leg}} \sum_{m,\nu} \left[\frac{1}{2}(S^+_{m,\nu} S^-_{m+1,\nu} + \text{H.c.}) + \Delta S^z_{m,\nu} S^z_{m+1,\nu} \right] \quad (1)$$

describing the coupling along the rungs and legs, respectively. The sites are labeled by (m,ν), where $m \in \{1,\ldots,L\}$ denotes the position within chain $\nu = 1,2$. All spin-1/2 operators are taken to be dimensionless such that J_{rung}, J_{leg} have dimensions of energy, and Δ is a dimensionless XXZ anisotropy parameter. In the following we will always assume a ladder of length L with periodic boundary conditions if not specified otherwise. In the following we limit our discussion to the antiferromagnetic regime $J_{\text{leg}}, J_{\text{rung}} \geqslant 0$. Apart from the special case $J_{\text{leg}} = 1$, $J_{\text{rung}} = 0$ (corresponding to two decoupled critical $S = 1/2$ chains), the system is gapped in this regime, with exponentially decaying correlations.

II. EXACT DIAGONALIZATION RESULTS

Before discussing our analytical results in the two limiting cases we present an overview of the full $J_{\text{leg}}/J_{\text{rung}}$ dependence of the entanglement spectrum $\xi := -\log(\lambda)$ obtained from the eigenvalues λ of the reduced density matrix of a single chain in a Heisenberg ($\Delta = 1$) spin ladder (cf. bipartition setup shown in Fig. 1). In the region $J_{\text{leg}}/J_{\text{rung}} < 1$ selected numerical spectra have already been presented in Refs. 17 and 20.

In the upper panel of Fig. 2 the bare entanglement spectrum for an $L = 8$ ladder is shown as a function of $J_{\text{leg}}/J_{\text{rung}}$ (note the logarithmic x axis), where the levels are labeled according to their S^z quantum number.[28] In the limit $J_{\text{leg}}/J_{\text{rung}} \to 0^+$ all the 2^L levels of the entanglement spectrum collapse onto a single value $L \ln 2$, and for finite $J_{\text{leg}}/J_{\text{rung}}$ they start to spread. For $J_{\text{leg}}/J_{\text{rung}} \gtrsim 1$ the spectrum rearranges, and a notable

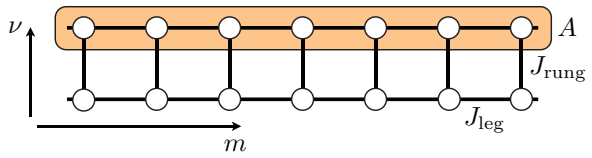

FIG. 1. (Color online) Two-leg spin ladder considered in this paper. The chains are labeled by $\nu = 1,2$, while the runs are labeled by $m = 1, \ldots L$. We consider the entanglement spectrum in the illustrated chain-chain bipartition.

feature is that the lowest levels above the singlet ground states are a sizable set of $S = 1$ triplets, displaying a common slope of 2 when plotted as a function of $\ln(J_{\rm leg}/J_{\rm rung})$. Note that this is in contrast with the behavior at small $J_{\rm leg}/J_{\rm rung}$, where there is only one triplet located below the second singlet in the entanglement spectrum.

In the lower panels of Fig. 2 we highlight the behavior in the two limit cases by appropriately rescaling and shifting the entanglement spectra. In the lower left panel we also show the energy spectrum of an $L = 8$ Heisenberg chain (multiplied by two) to demonstrate the remarkable agreement between the entanglement spectrum and the energy spectrum in this particular limit. As just discussed the structure of the entanglement spectrum is somewhat different in the opposite limit, and the analogy with the energy spectrum of a single chain apparently breaks down.

We now provide an analytical justification of the reported behavior based on perturbation theory around the two limits (a) and (b) described above.

III. Strong rung coupling limit

Let us now treat $\mathcal{H}_1$ as a perturbation to $\mathcal{H}_0$ with antiferromagnetic coupling, $J_{\rm rung} > 0$. The unperturbed ground state reads

$$|0\rangle = \bigotimes_m |s_m\rangle, \tag{2}$$

using obvious notation for singlet and triplet states on the rungs,

$$|s_m\rangle = \frac{1}{\sqrt{2}}(|\uparrow\rangle_{m,1}\,|\downarrow\rangle_{m,2} - |\downarrow\rangle_{m,1}\,|\uparrow\rangle_{m,2}), \tag{3}$$

$$|t_m^+\rangle = |\uparrow\rangle_{m,1}\,|\uparrow\rangle_{m,2}, \tag{4}$$

$$|t_m^0\rangle = \frac{1}{\sqrt{2}}(|\uparrow\rangle_{m,1}\,|\downarrow\rangle_{m,2} + |\downarrow\rangle_{m,1}\,|\uparrow\rangle_{m,2}), \tag{5}$$

$$|t_m^-\rangle = |\downarrow\rangle_{m,1}\,|\downarrow\rangle_{m,2}. \tag{6}$$

A. First order

The first-order correction to the ground state can be obtained by elementary calculation,

$$|1\rangle = +\frac{J_{\rm leg}}{4J_{\rm rung}} \sum_m \Big[\frac{2}{1+\Delta}(\cdots |t_m^+\rangle|t_{m+1}^-\rangle\cdots) + \frac{2}{1+\Delta}(\cdots |t_m^-\rangle|t_{m+1}^+\rangle\cdots) - \Delta\big(\cdots |t_m^0\rangle|t_{m+1}^0\rangle\cdots\big)\Big], \tag{7}$$

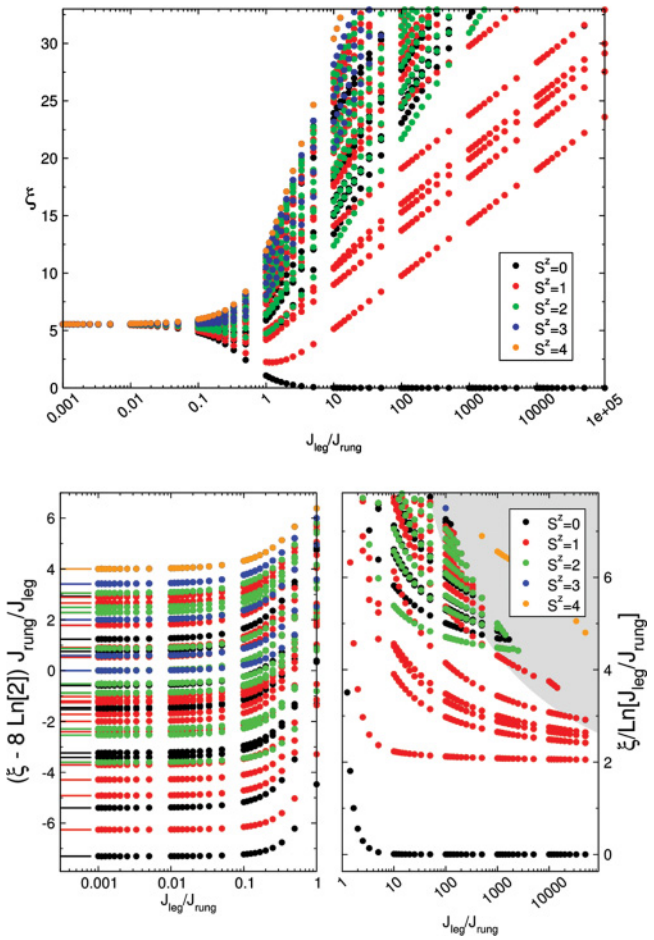

FIG. 2. (Color online) Overview of the entanglement spectrum of the reduced density matrix of a single chain (cf. setup in Fig. 1) in a Heisenberg ($\Delta = 1$) spin ladder for different $S^z_{\rm tot} = S_{\rm tot}$ sectors as a function of $J_{\rm leg}/J_{\rm rung}$. The system size is $L = 8$. While in the upper panel the bare entanglement spectrum is shown, in the lower panels the leading asymptotic behavior in the two limiting cases $J_{\rm leg}/J_{\rm rung} \to 0$ and $J_{\rm rung}/J_{\rm leg} \to 0$ is highlighted by appropriate shifts and rescaling indicated on the y axes. The filled dots in all panels denote numerical entanglement spectrum levels, while the constant lines in the lower left panel highlight twice the eigenvalues of a single $L = 8$, $S = 1/2$ Heisenberg chain. The gray region in the lower right panel indicates the part of the rescaled entanglement spectrum affected by the finite (double) precision arithmetic used in the numerical calculations.

where the dots denote singlet states on each rung not explicitly specified. The reduced density operator is obtained by tracing out one of the legs from $\rho = (|0\rangle + |1\rangle)(\langle 0| + \langle 1|)$ and is given within first order in $J_{\rm leg}/J_{\rm rung}$ by

$$\rho_{\rm red}^{(1)} = \frac{1}{2^L}\Bigg(1 - \frac{4J_{\rm leg}}{J_{\rm rung}(1+\Delta)} \sum_m \Big[(S_m^+ S_{m+1}^- + \text{H.c.}) + \frac{1}{2}(\Delta + \Delta^2)\, S_m^z S_{m+1}^z\Big]\Bigg), \tag{8}$$

with L being the number of rungs. Again within first-order perturbation theory, this result can be formulated as

$$\rho_{\rm red}^{(1)} = \frac{1}{Z}\exp\big(-\mathcal{H}_{\rm ent}^{(1)}\big), \tag{9}$$

with $Z = \mathrm{Tr}\,\exp(-\mathcal{H}^{(1)}_{\mathrm{ent}})$ being a partition function. The entanglement Hamiltonian[2] $\mathcal{H}^{(1)}_{\mathrm{ent}}$ is given as

$$\mathcal{H}^{(1)}_{\mathrm{ent}} = \frac{4}{1+\Delta}\frac{J_{\mathrm{leg}}}{J_{\mathrm{rung}}} \times \sum_m \left[\frac{1}{2}(S^+_m S^-_{m+1} + \mathrm{H.c.}) + \tilde{\Delta} S^z_m S^z_{m+1}\right], \quad (10)$$

and is of nearest-neighbor XXZ form, with a renormalized anisotropy parameter,

$$\tilde{\Delta} = \tfrac{1}{2}(\Delta + \Delta^2). \quad (11)$$

Note that $\Delta = 0$ (XX case) and $\Delta = 1$ (Heisenberg interactions) are invariant, i.e., the entanglement Hamiltonian is proportional to the physical Hamiltonian restricted to the block, as observed numerically for $\Delta = 1$ earlier in Ref. 17. Since in these two specific cases the physical Hamiltonian on a chain and the entanglement Hamiltonian are simply proportional to each other (to first order), one can define an *ad hoc* inverse temperature

$$\beta = \frac{4}{1+\Delta}\frac{J_{\mathrm{leg}}}{J_{\mathrm{rung}}}, \quad (12)$$

such that $\mathcal{H}^{(1)}_{\mathrm{ent}} = \beta\,\hat{\mathcal{H}}_{XXZ}$, with a $J_{\mathrm{leg}}/J_{\mathrm{rung}}$ dependence solely in β.

B. Second order

The second-order contribution to the ground state is somewhat lengthy and given in the Appendix. For general anisotropy the result does not seem to be amenable to a simple interpretation. In the isotropic case $\Delta = 1$, however, one finds up to second order,

$$\rho^{(2)}_{\mathrm{red}} = \frac{1}{2^L}\left\{1 - \frac{2J_{\mathrm{leg}}}{J_{\mathrm{rung}}}\sum_m \vec{S}_m\vec{S}_{m+1} + \frac{1}{2}\left(\frac{2J_{\mathrm{leg}}}{J_{\mathrm{rung}}}\right)^2\left(\left[\sum_m \vec{S}_m\vec{S}_{m+1}\right]^2 - \frac{3}{16}L + \frac{1}{4}\sum_m[\vec{S}_m\vec{S}_{m+2} - \vec{S}_m\vec{S}_{m+1}]\right)\right\}, \quad (13)$$

which can, within the same order, be reformulated as

$$\rho^{(2)}_{\mathrm{red}} = \frac{1}{Z}\exp\left(-\mathcal{H}^{(2)}_{\mathrm{ent}}\right), \quad (14)$$

with $Z = \mathrm{Tr}\,\exp(-\mathcal{H}^{(2)}_{\mathrm{ent}})$ and

$$\mathcal{H}^{(2)}_{\mathrm{ent}} = 2\frac{J_{\mathrm{leg}}}{J_{\mathrm{rung}}}\sum_m \vec{S}_m\vec{S}_{m+1} + \frac{1}{2}\left(\frac{J_{\mathrm{leg}}}{J_{\mathrm{rung}}}\right)^2\sum_m[\vec{S}_m\vec{S}_{m+1} - \vec{S}_m\vec{S}_{m+2}]. \quad (15)$$

Thus, also within second order $J_{\mathrm{leg}}/J_{\mathrm{rung}}$ the entanglement Hamiltonian is quite similar to the physical Hamiltonian on a single chain. The second-order correction contains a renormalization of the amplitude of the nearest-neighbor coupling and the appearance of an unfrustrated ferromagnetic next-nearest-neighbor Heisenberg coupling. The latter observation is in accordance with the numerical findings in Refs. 20 and 18. We expect this picture to hold also at higher order. According to general linked cluster ideas, sites at distance r will only be able to couple starting at order r with a leading amplitude proportional to $(\frac{J_{\mathrm{leg}}}{J_{\mathrm{rung}}})^r$. Given the Heisenberg nature of the leg interactions, to leading order a Heisenberg interaction $\sum_m \vec{S}_m\vec{S}_{m+r}$ is the only symmetry-allowed interaction.

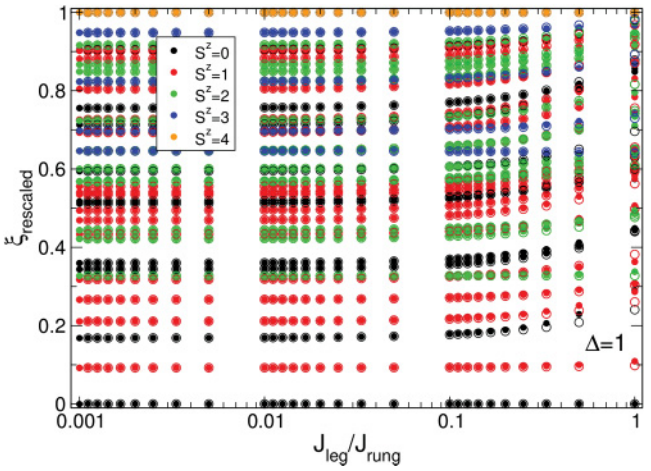

FIG. 3. (Color online) Filled circles: numerical entanglement spectra obtained for an $L = 8$ system. For each $J_{\mathrm{leg}}/J_{\mathrm{rung}}$ value the entanglement spectrum has been rescaled to lie in the interval [0,1]. Empty circles: rescaled energy spectrum of the analytical second-order entanglement Hamiltonian, Eq. (15).

In Fig. 3 we present a comparison between the rescaled numerical entanglement spectra for $L = 8$ and the perturbative result in the form of the energy spectrum of Eq. (15) for $J_{\mathrm{leg}}/J_{\mathrm{rung}} \leqslant 1$. The second-order corrections only seem to become visible for this system size for $J_{\mathrm{leg}}/J_{\mathrm{rung}} \gtrsim 0.1$, and the initial deviations from a straight line in the numerics are correctly described by the second-order corrections. However, for larger $J_{\mathrm{leg}}/J_{\mathrm{rung}}$ ratios further neighbor Heisenberg couplings and multispin interactions become non-negligible, as observed in Ref. 20.

IV. LIMIT OF WEAKLY COUPLED CHAINS

We now discuss the opposite limit of weakly coupled chains. At the starting point $J_{\mathrm{rung}}/J_{\mathrm{leg}} = 0$ the ground state is the product of the ground states of the individual chains.

$$|\psi_0\rangle = |0\rangle_A|0\rangle_B. \quad (16)$$

In this limit the entanglement spectrum is trivial, composed of only a single value $\xi = 0$.

To first order the wave function reads

$$|\psi_1\rangle = [1 - RQ_0\mathcal{H}_0]|\psi_0\rangle, \quad (17)$$

where $\mathcal{H}_0$ is the Hamiltonian coupling the two chains [cf. Eq. (1)], Q_0 is the projector onto the subspace orthogonal to $|\psi_0\rangle$, and R denotes the resolvent operator $R = (\mathcal{H}_1 - E_0)^{-1}$.[29]

After a straightforward calculation one obtains the following expression for the first-order wave function $|\psi_1\rangle$ in the product basis of chain eigenfunctions:

$$|\psi_1\rangle = |0\rangle_A|0\rangle_B + \frac{\Delta\, J_{\rm rung}}{J_{\rm leg}} \sum_k \sum_{n,n'\neq 0} \frac{\langle n|S^z_k|0\rangle_A \langle n'|S^z_{-k}|0\rangle_B}{\Delta_n + \Delta_{n'}} |n\rangle_A|n'\rangle_B + \frac{J_{\rm rung}}{J_{\rm leg}} \sum_{k;\alpha\in\{x,y\}} \sum_{n,n'\neq 0} \frac{\langle n|S^\alpha_k|0\rangle_A \langle n'|S^\alpha_{-k}|0\rangle_B}{\Delta_n + \Delta_{n'}} |n\rangle_A|n'\rangle_B \quad (18)$$

$$= \sum_{n,n'} [\psi_1]_{n,n'} |n\rangle_A|n'\rangle_B, \quad (19)$$

where k runs over the lattice momenta of a single chain, α runs over the spin components $\{x,y\}$, n and n' label the eigenfunctions of the two isolated chains, while $\Delta_{n(n')}$ denotes the single-chain excitation energies $E_{n(n')} - E_0$. One recognizes that the nontrivial part of the wave function is composed of contributions which also enter the Lehmann representation of the $\mathcal{S}^{\alpha\alpha}(k,\omega)$ spectral functions of a single chain,

$$\mathcal{S}^\alpha(k,\omega) = \sum_n \left|c^{k,\alpha}_n\right|^2 \delta(\omega - \Delta_n), \quad (20)$$

$$c^{k,\alpha}_n = \langle n|S^\alpha_k|0\rangle, \quad (21)$$

where the matrix elements $c^{k,\alpha}_n$ enter as

$$[\psi_1]_{n,n'} = \delta_{n,0}\delta_{n',0} + \frac{\Delta J_{\rm rung}}{J_{\rm leg}} \sum_k \frac{c^{k,z}_n c^{k,z}_{n'}}{\Delta_n + \Delta_{n'}} + \frac{1}{2}\frac{J_{\rm rung}}{J_{\rm leg}} \sum_k \frac{c^{k,+}_n c^{-k,-}_{n'}}{\Delta_n + \Delta_{n'}} + \frac{1}{2}\frac{J_{\rm rung}}{J_{\rm leg}} \sum_k \frac{c^{k,-}_n c^{-k,+}_{n'}}{\Delta_n + \Delta_{n'}}. \quad (22)$$

Given the wave function in this form, the entanglement spectrum can simply be obtained by a singular value decomposition of the matrix $[\psi_1]_{n,n'}$, which amounts to finding the Schmidt decomposition in this bipartition. The singular values are thus the Schmidt values, and when squared they correspond to the eigenvalues of the reduced density matrix in the same bipartition setup. Due to the translational invariance along the chains as well as the total S^z-preserving form of the XXZ Hamiltonians, the wave-function matrix exhibits a block-diagonal structure in k and only n and n' sectors with total $S^z = 0, \pm 1$ appear. In the specific case of Heisenberg Hamiltonians ($\Delta = 1$) one can then infer by virtue of the Wigner-Eckart theorem that only total spin $S = 1$ entanglement levels appear above the singlet ground state to leading order. In addition, the singlet ground state leads to vanishing spectral weight at $k = 0$ and therefore the absence of $S = 1$ entanglement levels at $k = 0$ to the expansion order considered.

In Fig. 4 we show a comparison between the numerical entanglement spectrum for $L = 8$ at $J_{\rm rung}/J_{\rm leg} = 0.0001$ and the prediction based on Eq. (22). The filled symbols represent *all* the predicted entanglement levels appearing at this order. The numerical results match perfectly the analytical prediction up to the finite precision threshold of the numerics.

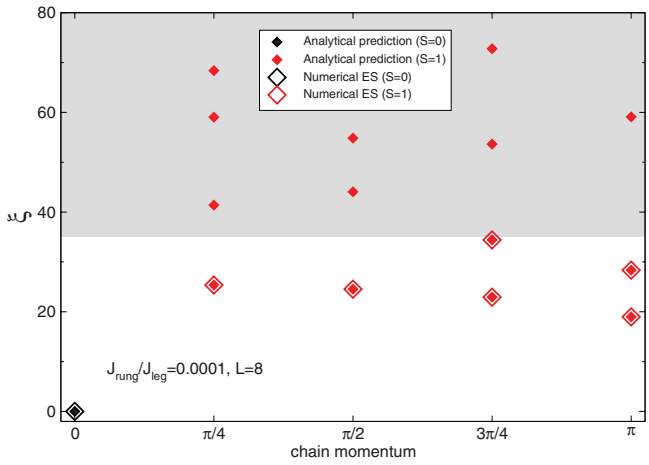

FIG. 4. (Color online) Filled diamonds: entanglement spectrum prediction for an $L = 8$ Heisenberg spin ladder, based on the first-order perturbation theory in the coupling between the two chains Eq. (22). Empty diamonds: $S = 0$ and $S = 1$ entanglement levels obtained from exact diagonalization at $J_{\rm rung}/J_{\rm leg} = 0.0001$ (cf. upper panel of Fig. 2). The gray region denotes the region where the numerical entanglement spectrum is affected by the finite precision arithmetics and where no numerical data is shown.

V. DISCUSSION AND CONCLUSION

In summary, we have investigated the entanglement spectra of spin-1/2 XXZ ladders using both exact numerical diagonalizations and perturbation theory approaches. In the limit of strong rung coupling, perturbation theory predicts in leading order an entanglement Hamiltonian being also of nearest-neighbor XXZ form with a renormalized anisotropy parameter. For XX and isotropic Heisenberg ladders no such renormalization takes place and in this case one can define an *ad hoc* effective temperature proportional to the $J_{\rm rung}/J_{\rm leg}$ ratio. Moreover, in next-to-leading order the entanglement Hamiltonian exhibits spin couplings of longer range, and all the above findings are in perfect agreement with our numerical exact diagonalization results. The first-order perturbation theory result has also been obtained in parallel work by Peschel and Chung.[18] Similar numerical observations have already been made for quantum Hall bilayers at filling factor $\nu = 1$.[12] It remains an open task to devise analogous perturbational arguments for such systems with long-ranged interactions.

In the opposite regime of strong coupling along the legs, we point out an interesting connection of the entanglement spectrum to the Lehmann representation of single-chain spectral functions of the operators contained in the physical Hamiltonian coupling the two chains. This aspect also holds true for other ladder systems, such as, e.g., Hubbard ladders, where the entanglement spectrum will be determined by elements of the single-particle addition and removal of spectral functions in the weakly coupled chain regime.

ACKNOWLEDGMENTS

A.M.L. thanks V. Alba and M. Haque for collaboration on related topics. The work of J.S. was supported by DFG via SFB631.

APPENDIX: SECOND-ORDER CORRECTION TO THE GROUND STATE AND THE REDUCED DENSITY MATRIX

The second-order correction to the ground state can be obtained as

$$
\begin{aligned}
|2\rangle = & \left(\frac{J_{\text{leg}}}{J_{\text{rung}}}\right)^2 \sum_{|m-n|>1} \Bigg[\frac{1}{4(1+\Delta)^2} \left(|t_m^+, t_{m+1}^-, t_n^+, t_{n+1}^-\rangle + |t_m^+, t_{m+1}^-, t_n^-, t_{n+1}^+\rangle\right) \\
& - \frac{\Delta}{4(3+\Delta)} \left(\frac{1}{2} + \frac{1}{1+\Delta}\right) \left(|t_m^+, t_{m+1}^-, t_n^0, t_{n+1}^0\rangle + |t_m^-, t_{m+1}^+, t_n^0, t_{n+1}^0\rangle\right) + \frac{\Delta^2}{32} |t_m^0, t_{m+1}^0, t_n^0, t_{n+1}^0\rangle \Bigg] \\
& + \left(\frac{J_{\text{leg}}}{J_{\text{rung}}}\right)^2 \sum_m \Bigg[-\frac{1}{2(1+\Delta)^2} \left(|t_m^+, t_{m+2}^-\rangle + |t_m^-, t_{m+2}^+\rangle\right) + \frac{\Delta^2}{8} |t_m^0, t_{m+2}^0\rangle \Bigg] \\
& + \left(\frac{J_{\text{leg}}}{J_{\text{rung}}}\right)^2 \sum_m \Bigg[\frac{\Delta}{8(1+\Delta)} \left(\frac{1}{2} + \frac{1}{1+\Delta}\right) \left(|t_m^+, t_{m+1}^-\rangle + |t_m^-, t_{m+1}^+\rangle\right) - \frac{1}{4(1+\Delta)} |t_m^0, t_{m+1}^0\rangle \Bigg] \\
& - \left(\frac{J_{\text{leg}}}{J_{\text{rung}}}\right)^2 \frac{L}{8} \left(\frac{2}{(1+\Delta)^2} + \frac{\Delta^2}{4}\right) |0\rangle. \qquad \text{(A1)}
\end{aligned}
$$

Note that no terms with an odd number of triplets occur. In the isotropic Heisenberg case $\Delta = 1$, the second-order contribution to the reduced density matrix is the sum of the following expressions:

$$
\text{Tr}_{1\text{ leg}} \left(|0\rangle\langle 2| + |2\rangle\langle 0|\right) = \left(\frac{J_{\text{leg}}}{J_{\text{rung}}}\right)^2 \frac{1}{2^L} \left(\sum_{|m-n|>1} (\vec{S}_m \vec{S}_{m+1})(\vec{S}_n \vec{S}_{n+1}) + \sum_m [\vec{S}_m \vec{S}_{m+2} - \vec{S}_m \vec{S}_{m+1}] - \frac{3}{16} L \right), \qquad \text{(A2)}
$$

$$
\text{Tr}_{1\text{ leg}} \left(|1\rangle\langle 1|\right) = \left(\frac{J_{\text{leg}}}{J_{\text{rung}}}\right)^2 \frac{1}{2^L} \left(\sum_{|m-n|>1} (\vec{S}_m \vec{S}_{m+1})(\vec{S}_n \vec{S}_{n+1}) + \frac{1}{2} \sum_m [\vec{S}_m \vec{S}_{m+2} - \vec{S}_m \vec{S}_{m+1}] + \frac{3}{16} L \right). \qquad \text{(A3)}
$$

Now using the identities

$$
\tfrac{1}{2} \vec{S}_1 \vec{S}_3 = (\vec{S}_1 \vec{S}_2)(\vec{S}_2 \vec{S}_3) + (\vec{S}_2 \vec{S}_3)(\vec{S}_1 \vec{S}_2) \qquad \text{(A4)}
$$

and

$$
\tfrac{3}{16} - \tfrac{1}{2} \vec{S}_1 \vec{S}_2 = (\vec{S}_1 \vec{S}_2)^2 \qquad \text{(A5)}
$$

for spin-1/2 operators, one derives the result (13).

*andreas.laeuchli@uibk.ac.at
†john.schliemann@physik.uni-regensburg.de

[1] L. Amico, R. Fazio, A. Osterloh, and V. Vedral, Rev. Mod. Phys. **80**, 517 (2008).
[2] H. Li and F. D. M. Haldane, Phys. Rev. Lett. **101**, 010504 (2008).
[3] N. Regnault, B. A. Bernevig, and F. D. M. Haldane, Phys. Rev. Lett. **103**, 016801 (2009).
[4] O. S. Zozulya, M. Haque, and N. Regnault, Phys. Rev. B **79**, 045409 (2009).
[5] A. M. Läuchli, E. J. Bergholtz, J. Suorsa, and M. Haque, Phys. Rev. Lett. **104**, 156404 (2010).
[6] R. Thomale, A. Sterdyniak, N. Regnault, and B. A. Bernevig, Phys. Rev. Lett. **104**, 180502 (2010).
[7] A. Sterdyniak, N. Regnault, and B. A. Bernevig, Phys. Rev. Lett. **106**, 100405 (2011).
[8] R. Thomale, B. Estienne, N. Regnault, and B. A. Bernevig, Phys. Rev. B **84**, 045127 (2011).
[9] A. Chandran, M. Hermanns, N. Regnault, and B. A. Bernevig, Phys. Rev. B **84**, 205136 (2011).
[10] A. Sterdyniak, B. A. Bernevig, N. Regnault, and F. D. M. Haldane, New J. Phys. **13**, 105001 (2011).
[11] X.-L. Qi, H. Katsura, and A. W. W. Ludwig, e-print arXiv:1103.5437 (to be published).
[12] J. Schliemann, Phys. Rev. B **83**, 115322 (2011).
[13] P. Calabrese and A. Lefevre, Phys. Rev. A **78**, 032329 (2008).
[14] F. Pollmann and J. E. Moore, New J. Phys. **12**, 025006 (2010).
[15] F. Pollmann, A. M. Turner, E. Berg, and M. Oshikawa, Phys. Rev. B **81**, 064439 (2010).
[16] R. Thomale, D. P. Arovas, and B. A. Bernevig, Phys. Rev. Lett. **105**, 116805 (2010).
[17] D. Poilblanc, Phys. Rev. Lett. **105**, 077202 (2010).
[18] I. Peschel and M.-C. Chung, EPL **96**, 50006 (2011).
[19] H. Yao and X.-L. Qi, Phys. Rev. Lett. **105**, 080501 (2010).
[20] J. I. Cirac, D. Poilblanc, N. Schuch, and F. Verstraete, Phys. Rev. B **83**, 245134 (2011).
[21] C.-Y. Huang and F. L. Lin, Phys. Rev. B **84**, 125110 (2011).
[22] L. Fidkowski, Phys. Rev. Lett. **104**, 130502 (2010).
[23] E. Prodan, T. L. Hughes, and B. A. Bernevig, Phys. Rev. Lett. **105**, 115501 (2010).
[24] Z. Liu, H.-L. Guo, V. Vedral, and H. Fan, Phys. Rev. A **83**, 013620 (2011).

[25]S. Furukawa and Y.-B. Kim, Phys. Rev. B **83**, 085112 (2011).
[26]X. Deng and L. Santos, Phys Rev. B **84**, 085138 (2011).
[27]J. Dubail and N. Read, Phys. Rev. Lett. **107**, 157001 (2011).
[28]In the chain-chain bipartition setup the chain momentum is also a good quantum number, but we do not use this quantum number here for the sake of a simple presentation.
[29]For a finite system the perturbation theory is expected to have a finite radius of convergence.